

# Spontaneous Parametric Down-Conversion and Quantum Walks in Arrays of Quadratic Nonlinear Waveguides

Alexander S. Solntsev, Andrey A. Sukhorukov, Dragomir N. Neshev, and Yuri S. Kivshar  
*Nonlinear Physics Center and Center for Ultrahigh Bandwidth Devices for Optical Systems (CUDOS),  
Research School of Physics and Engineering, Australian National University,  
Canberra ACT 0200, Australia*

(Received 27 April 2011; published 10 January 2012)

We analyze the process of photon-pair generation with simultaneous quantum walks in a quadratic nonlinear waveguide array. We demonstrate that the spontaneous parametric down-conversion in the array allows for creating quantum states with strongly pronounced spatial correlations, which are qualitatively different from those possible in bulk crystals or through quantum walks in linear waveguide arrays. Most importantly, the photon correlations can be controlled entirely classically by varying the spatial profile of the pump beam or the phase-matching conditions.

DOI: [10.1103/PhysRevLett.108.023601](https://doi.org/10.1103/PhysRevLett.108.023601)

PACS numbers: 42.50.Dv, 42.50.Ar, 42.65.Lm, 42.82.Et

Spontaneous parametric down-conversion (SPDC) is probably the most commonly used process for generation of quantum correlated photons [1] with many applications including quantum cryptography [2] and quantum logic devices [3,4]. However, the use of bulk optics for generating correlated photons as well as for the building blocks of logic gates hinders the scalability of the quantum circuitry with an increasing number of components. Indeed, the successful operation of a quantum optical circuit requires that the fidelity of the quantum interference, which lies at the heart of single-photon interactions, is preserved after passing through all optical components. Integrated optical quantum circuits are seen as a solution for on-chip scalable quantum networks with important demonstrations of multiphoton entanglement [5], quantum factoring algorithms [6], and polarization entanglement [7]. Additionally, integrated circuits are compact and stable and could lead in the near future to mass production of chips for quantum computation.

A particularly important building block for quantum manipulation and integrated nonclassical light is the directional coupler formed by two coupled waveguides. A waveguide coupler can act as a simple beam splitter, thus opening numerous opportunities for integration of multiple photon gates [5]. The increase of the number of “beam splitters” can thus be simply realized by the addition of multiple coupled waveguides on a chip, leading ultimately to an array of coupled optical waveguides [8]. Waveguide arrays have been used to perform quantum walks of photon pairs resulting in nontrivial quantum correlations at the array output [9,10]. Such a kind of correlated walks involving quantum interference of several walkers can provide a speed-up of quantum algorithms delivering an exponential acceleration with the number of correlated walkers [11,12]. However, in all schemes to date, the correlated photon pairs were generated externally to the array by using bulk photonic elements. Such bulk elements

may introduce quantum decoherence and impose stringent requirements on the losses associated with the connection of the array to the photon sources.

In this Letter, we propose and demonstrate numerically a novel scheme of quantum walks, involving simultaneous generation of correlated photon pairs through SPDC and their quantum walks inside a single photonic element—an array of quadratic nonlinear waveguides. This scheme avoids entirely the need for complex interfaces required in previous experiments [10] but, most importantly, enables novel ways for control of the spatial quantum correlations at the array output. In particular, we show that by varying the phase-matching conditions for the SPDC process or the spatial profile of the pump beam it is possible to control the output quantum states incorporating photon bunching or antibunching. Importantly, such simple yet flexible control of quantum statistics is not possible when the photon pairs are created externally to the array. Although integrated photonic couplers [13,14] and circuits [15] incorporating SPDC were proposed previously, we emphasize that integrating SPDC and quantum walks in a single nonlinear array leads to additional quantum interference between probabilities to generate photon pairs in different places of the array. This quantum interference is vital in order to improve the clarity of output spatial correlations.

Arrays of quadratic nonlinear waveguides have been widely explored for manipulation of optical pulses through cascaded generation of the second harmonic [8]. Here, we consider the reversed SPDC process and study the generation of correlated photon pairs as schematically illustrated in Fig. 1(a). To demonstrate the flexibility in controlling photon states, we consider a phase-matched near-degenerate type-I SPDC, when a pump beam generates signal and idler photons of the same polarization and frequencies approximately half of the pump beam frequency. Whereas nondegenerate SPDC can also occur in

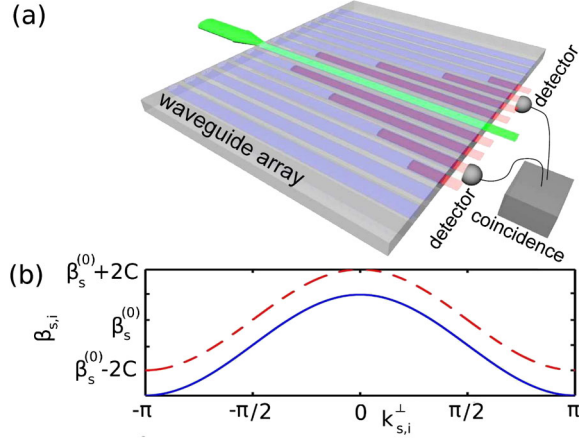


FIG. 1 (color online). (a) Schematic of a quadratic waveguide array: The pump beam generates photon pairs that couple to the neighboring waveguides. (b) Propagation constant vs normalized transverse wave number for the near-degenerate signal (red dashed line) and idler (blue solid line).

the array, it can be excluded through frequency filtering at the output.

The quantum walks in the array can occur due to photon tunneling between waveguides, and we consider a common case when such tunneling occurs between neighboring waveguides and its rate can be characterized by the coupling coefficients  $C_{s,i}$  [8,10], where subscripts  $s$  and  $i$  denote signal and idler waves, respectively. We consider the filtered frequency range to be sufficiently narrow such that the coupling coefficients are essentially the same for the signal and idler photons and denote  $C \equiv C_{s,i}$ .

For homogeneous waveguide arrays, it is convenient to represent photon states through a basis of extended Bloch waves (conceptually analogous to Fourier plane-wave expansion in bulk crystals) which have the form  $\exp(ik_{s,i}^{\perp}n + i\beta_{s,i}z)$  [8]. Here  $n$  is the waveguide number,  $k_{s,i}^{\perp}$  are the normalized transverse wave numbers which define the phase difference between the neighboring waveguides, and  $\beta_{s,i}$  are the propagation constants which define the longitudinal wave numbers. Then, the spatial dispersion follows a general relation for waveguide arrays [8]:

$$\beta_{s,i} = \beta(\omega_{s,i}, k_{s,i}^{\perp}) = \beta^{(0)}(\omega_{s,i}) + 2C \cos(k_{s,i}^{\perp}). \quad (1)$$

Here  $\beta^{(0)}$  is a propagation constant for a single waveguide, and  $\omega_{s,i}$  are frequencies of signal and idler waves. We plot the characteristic dispersion curves for the signal and idler waves in Fig. 1(b). For a pump beam with optical frequency  $\omega_p \approx 2\omega_{s,i}$ , a dispersion relation analogous to Eq. (1) will also apply; however, the corresponding coupling coefficient  $C_p$  would generally have a much smaller value compared to the signal and idler waves,  $C_p \ll C$ , due to the weaker mode overlap between neighboring waveguides at higher frequencies [8]. In practice,  $C_p L \ll 1$ , where  $L$  is the array length, and therefore the coupling

effects can be neglected for the pump beam ( $C_p \approx 0$ ). In this case, the input pump beam profile  $A_n(n)$  remains constant inside the array.

We emphasize that the spatial dispersion for the waveguide arrays is very different from bulk crystals. First, in bulk structures the rate of diffraction is proportional to the light wavelength inside the material. In particular, the pump beam diffraction is roughly one-half of the diffraction experienced by the near-degenerate signal and idler waves. In contrast, in waveguide arrays, the rate of signal and idler diffraction is defined by the coupling  $C$ , which can be flexibly engineered, for example, by varying the transverse waveguide separation. At the same time, the pump diffraction can be practically suppressed as we discussed above. Second, in bulk media, the spatial dispersion is parabolic in the paraxial regime,  $\beta \approx -D(k^{\perp})^2$ . As such, for each wave number there is a unique propagation direction defined by the normalized propagation angle as  $\nu(k^{\perp}) = -\partial\beta/\partial k^{\perp} = 2Dk^{\perp}$ . In arrays, the dispersion shape is very different [Eq. (1)], and, in particular, there appear pairs of waves with different wave numbers yet the same propagation directions since [8]  $\nu(k^{\perp}) = 2C \sin(k^{\perp})$  and  $\nu(k^{\perp}) \equiv \nu(\pi - k^{\perp})$ . We show in the following that, due to these differences, the SPDC process in arrays can have new and unique features compared to bulk crystals.

We now study photon correlations at the array output by adopting the mathematical approach of Refs. [16–18]. We consider a continuous wave, narrow-band pump at central frequency  $\omega_p^{(0)}$  and describe the photon states at the array output by using the extended Bloch wave formalism, where the complete set of Bloch waves can be defined by the transverse wave numbers from the first Brillouin zone,  $-\pi \leq k^{\perp} < \pi$ . Then the expression for the two-photon state can be written as follows [19]:

$$|\psi\rangle = 2\pi B \int_{-\pi}^{\pi} dk_s^{\perp} dk_i^{\perp} \int_{\Delta\omega_{\min}}^{\Delta\omega_{\max}} d\Delta\omega |\Psi_k(k_s^{\perp}, k_i^{\perp}, \Delta\omega)\rangle, \quad (2)$$

where

$$\begin{aligned} |\Psi_k(k_s^{\perp}, k_i^{\perp}, \Delta\omega)\rangle &= A_k(k_s^{\perp} + k_i^{\perp}) \text{sinc}(\Delta\beta L/2) \\ &\quad \times \exp(-i\Delta\beta L/2) \hat{a}^{\dagger}(\Delta\omega, k_s^{\perp}) \hat{a}^{\dagger} \\ &\quad \times (-\Delta\omega, k_i^{\perp}) |0, 0\rangle. \end{aligned} \quad (3)$$

Here  $A_k$  is the  $k$ -space pump spectrum,  $B$  is a constant,  $k_{s,i}^{\perp}$  are the signal and idler normalized transverse wave numbers,  $(\Delta\omega_{\min}, \Delta\omega_{\max})$  is the wavelength range filtered for the measurement,  $\hat{a}^{\dagger}$  are photon creation operators at the specified transverse wave numbers and frequencies, and  $|0, 0\rangle$  is a vacuum state. We determine the phase mismatch by using Eq. (1):  $\Delta\beta(k_s^{\perp}, k_i^{\perp}, \Delta\omega) = \Delta\beta^{(0)}(\Delta\omega) - 2C \cos(k_s^{\perp}) - 2C \cos(k_i^{\perp})$ , where  $\Delta\beta^{(0)}(\Delta\omega)$  is the mismatch in a single waveguide and  $\Delta\omega = \omega_s - \omega_p^{(0)}/2 = \omega_p^{(0)}/2 - \omega_i$  is the signal and idler frequency detuning from the degenerate frequency  $\omega_p^{(0)}/2$ . Further

discussions on the single waveguide phase mismatch  $\Delta\beta^{(0)}(\Delta\omega)$  related to a specific experimental platform can be found in Supplementary Materials [19].

We now calculate the second-order correlation function  $\Gamma_k(k_s, k_i) = \int d\Delta\omega (|\langle \Psi_k | \Psi_k \rangle|^2)$ , which defines correlations between photons with specific transverse wave numbers. In order to determine correlations for the signal and idler photons in real space (corresponding waveguide numbers  $n_s$  and  $n_i$ ), we apply the Fourier transform to Eq. (3) and obtain the real-space two-photon state  $|\Psi_n(n_s, n_i, \Delta\omega)\rangle$ . We then calculate the photon number correlation function  $\Gamma_n(n_s, n_i) = \int d\Delta\omega (|\langle \Psi_n | \Psi_n \rangle|^2)$ , which can be measured by scanning two detectors across the array output and measuring coincidences [10] [see Fig. 1(a)]. Below, we use realistic experimental parameters of LiNbO<sub>3</sub> waveguide array [20] with a total length  $L = 10/C$ . (See Supplementary Materials [19] for information on waveguide frequency dispersion and output spectral filtering.)

We first consider the case when the pump is coupled to the central waveguide  $n = 0$ , which corresponds to a constant spatial Fourier spectrum of the pump,  $A_k(k_s^\perp + k_i^\perp) = 1$ . In Fig. 2, we plot the photon correlations at the array output in  $k$  space and real space, considering degenerate phase matching for a single waveguide when  $\Delta\beta^{(0)}(\Delta\omega = 0) = 0$ . A square shape is formed for the  $k$ -space correlations [Fig. 2(a)], which indicates a pronounced correlation between the generated signal and idler photons with transverse wave numbers satisfying the relations  $k_s^\perp \pm k_i^\perp \approx \pm\pi$ . This shape appears because these wave numbers correspond to the most efficient phase-matched interactions with  $\Delta\beta = -2C \cos(k_s^\perp) - 2C \cos(k_i^\perp) = 0$  at  $\Delta\omega = 0$ . We note that at phase matching the photons in a pair would have the same or opposite propagation directions as  $\nu(k_s^\perp) \approx \pm\nu(k_i^\perp)$ . Indeed, the corresponding real-space correlations, shown in Fig. 2(b), reveal that the probability of detecting signal and idler photons in either the same waveguide ( $n_s = n_i$ , bunching) or opposite waveguides ( $n_s = -n_i$ , antibunching) is significantly higher compared to the other probabilities. The bunching and antibunching in the photon-pair correlations

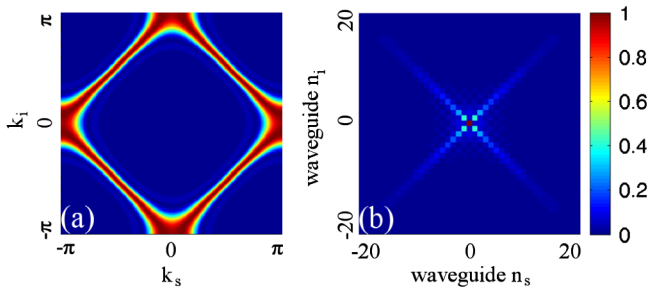


FIG. 2 (color online). Photon-pair correlations (a) in  $k$  space (spatial spectrum) and (b) in real space (waveguide numbers) for a pump coupled only to the central waveguide  $n = 0$  with zero single-waveguide degenerate phase mismatch.

are very strongly pronounced. This is attributed to the quantum interference of photon pairs generated at different places along the length of the central (input) waveguide. The interference increases the sharpness of correlations as long as the single-waveguide phase-matching conditions are met. However, if phase mismatch is introduced, the spatial correlations between the signal and idler photons start to degrade [19].

The output photon statistics can be tailored by changing the pump profile and phase. When the pump beam is coupled with equal amplitudes and phases to two neighboring waveguides,  $A_n(n) = 1$  for  $n = 0, 1$ , then the  $k$ -space correlation pattern is strongly modified [Fig. 3(a)] compared to the single-waveguide pump excitation. This happens because the pump spectrum is primarily concentrated in the central part of the Brillouin zone with  $|k_p| \leq \pi/2$ , and hence for phase-matched interactions  $k_p \approx k_s^\perp + k_i^\perp$ , this suppresses generation of photons with wave numbers  $k_s^\perp + k_i^\perp \approx \pm\pi$ . The remaining phase-matched processes with  $k_s^\perp - k_i^\perp \approx \pm\pi$  correspond to opposite velocities of generated photons since  $\nu(k_s^\perp) \approx -\nu(k_i^\perp)$ . Accordingly, the antibunching regime prevails in real space [Fig. 3(b)].

When we introduce a  $\pi$  phase difference between pump amplitudes in the input waveguides, i.e.,  $A_n(0) = 1$  and  $A_n(1) = \exp(i\pi) = -1$ , then the situation is effectively reversed with the other phase-matched processes dominant in  $k$  space. This leads to pronounced bunching statistics of biphotons in real space [Figs. 3(c) and 3(d)].

The output photon statistics can also be controlled by coupling the pump to spatially separated waveguides. The correlation distributions look especially interesting for the

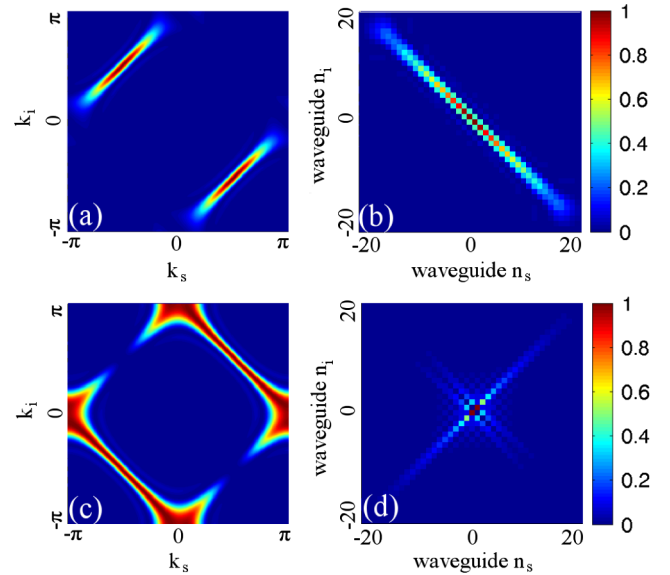


FIG. 3 (color online). Correlations of photon pairs (a),(c) in  $k$  space and (b),(d) in real space for single-waveguide degenerate phase mismatch equal to 0 and a pump coupled to waveguides  $n = 0, 1$  with amplitudes (a),(b)  $A_n(0) = A_n(1) = 1$  and (c),(d)  $A_n(0) = -A_n(1) = 1$ .

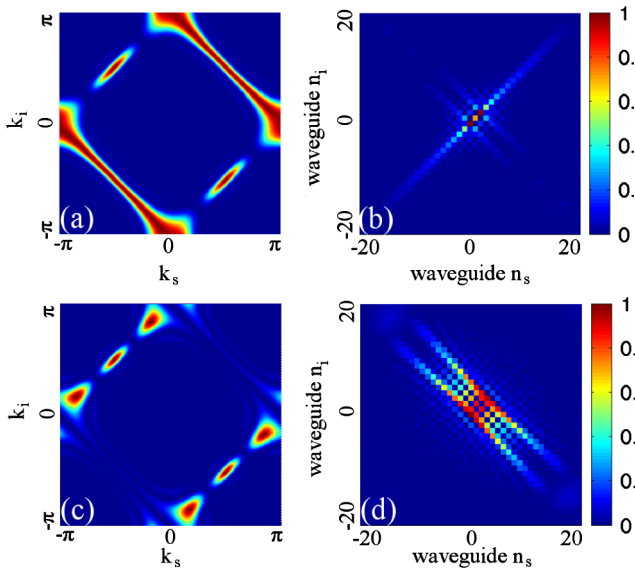


FIG. 4 (color online). Correlations of photon pairs (a),(c) in  $k$  space (spatial spectrum) and (b),(d) in real space (waveguide numbers) for a pump coupled to waveguides  $n = 0, 2$  (a),(b) and  $n = 0, 3$  (c),(d).

cases when waveguides  $n = 0, 2$  or  $n = 0, 3$  are excited by the pump beam. The output  $k$ -space interference patterns and real-space bunching or antibunching in this case depends on whether the number of nonpumped waveguides in between the pump inputs is even or odd; cf. Figs. 4(a)–4(d). This is analogous to the behavior previously observed in waveguide arrays with photon pairs coupled from an external source [9,10]; however, in the case of nonlinear waveguide arrays with combined SPDC and quantum walks, the correlations are much more pronounced due to the quantum interference between the probabilities to create photon pairs in different places along the length of the pumped waveguides.

In conclusion, we have studied the simultaneous SPDC and quantum walks in an array of quadratic nonlinear waveguides and have shown that the output correlations can be effectively controlled by changing the relative phase of the pump in two input waveguides, as well as by altering the phase mismatch for the SPDC process. Such control can enable careful engineering of the output quantum state, including dynamic switching from antibunching to bunching regimes. We have shown that SPDC in nonlinear waveguide arrays allows for strongly pronounced photon-pair correlations compared to quantum walks in linear arrays, owing to nontrivial interference between the probabilities to create photon pairs in different places along the length of the nonlinear array. In comparison to SPDC in bulk crystals, nonlinear waveguide arrays offer completely new opportunities for spatial dispersion control and accordingly for engineering different output quantum states.

We anticipate that our results may suggest new avenues for the development of quantum integrated circuits,

combining the generation of photon pairs and simultaneous transformation of the correlated photon states. We note that it was recently demonstrated that the spatial profiles of photon pairs generated during SPDC in bulk can be shaped by appropriate electric poling which modulates the sign of quadratic nonlinear susceptibility [21]. Quadratic nonlinear waveguide arrays can be also poled [8,20], and their flexibility in spatial dispersion control may allow one to match a wider range of specific application requirements in an integrated photonic platform. Nonlinear waveguide arrays can also become an attractive platform for the study of higher-dimensional quantum states. SPDC in bulk for these purposes requires careful path selection [22], while waveguide arrays intrinsically separate the generated photons in different waveguides. The generation of four-photon states in nonlinear waveguide arrays can be realized in relatively straightforward way by switching to type-II SPDC [23] and can also have interesting implications for quantum information processing.

We acknowledge useful discussions with G. Molina-Terriza, R. Schiek, M. Steel, and F. Setzpfandt, as well as support from the Australian Research Council.

- [1] S.P. Walborn, C.H. Monken, S. Padua, and P.H.S. Ribeiro, *Phys. Rep.* **495**, 87 (2010).
- [2] A.K. Ekert, J.G. Rarity, P.R. Tapster, and G.M. Palma, *Phys. Rev. Lett.* **69**, 1293 (1992).
- [3] J.L. O'Brien, G.J. Pryde, A.G. White, T.C. Ralph, and D. Branning, *Nature (London)* **426**, 264 (2003).
- [4] S. Gasparoni, J.W. Pan, P. Walther, T. Rudolph, and A. Zeilinger, *Phys. Rev. Lett.* **93**, 020504 (2004).
- [5] J.C.F. Matthews, A. Politi, A. Stefanov, and J.L. O'Brien, *Nature Photon.* **3**, 346 (2009).
- [6] A. Politi, J.C.F. Matthews, and J.L. O'Brien, *Science* **325**, 1221 (2009).
- [7] L. Sansoni, F. Sciarrino, G. Vallone, P. Mataloni, A. Crespi, R. Ramponi, and R. Osellame, *Phys. Rev. Lett.* **105**, 200503 (2010).
- [8] F. Lederer, G.I. Stegeman, D.N. Christodoulides, G. Assanto, M. Segev, and Y. Silberberg, *Phys. Rep.* **463**, 1 (2008).
- [9] Y. Bromberg, Y. Lahini, R. Morandotti, and Y. Silberberg, *Phys. Rev. Lett.* **102**, 253904 (2009).
- [10] A. Peruzzo, M. Lobino, J.C.F. Matthews, N. Matsuda, A. Politi, K. Poulios, X.Q. Zhou, Y. Lahini, N. Ismail, K. Worhoff, Y. Bromberg, Y. Silberberg, M.G. Thompson, and J.L. O'Brien, *Science* **329**, 1500 (2010).
- [11] N. Shenvi, J. Kempe, and K.B. Whaley, *Phys. Rev. A* **67**, 052307 (2003).
- [12] M. Hillery, D. Reitzner, and V. Buzek, *Phys. Rev. A* **81**, 062324 (2010).
- [13] Q. Zhang, X.P. Xie, H. Takesue, S.W. Nam, C. Langrock, M.M. Fejer, and Y. Yamamoto, *Opt. Express* **15**, 10288 (2007).
- [14] Q. Zhang, H. Takesue, C. Langrock, X.P. Xie, M.M. Fejer, and Y. Yamamoto, *Jpn. J. Appl. Phys.* **49**, 064401 (2010).

- [15] M. F. Saleh, G. Di Giuseppe, B. E. A. Saleh, and M. C. Teich, *IEEE Photon. J.* **2**, 736 (2010).
- [16] A. Christ, K. Laiho, A. Eckstein, T. Lauckner, P. J. Mosley, and C. Silberhorn, *Phys. Rev. A* **80**, 033829 (2009).
- [17] W. P. Grice and I. A. Walmsley, *Phys. Rev. A* **56**, 1627 (1997).
- [18] G. Di Giuseppe, M. Atature, M. D. Shaw, A. V. Sergienko, B. E. A. Saleh, and M. C. Teich, *Phys. Rev. A* **66**, 013801 (2002).
- [19] See Supplemental Material at <http://link.aps.org/supplemental/10.1103/PhysRevLett.108.023601> for theoretical derivations, details of possible experimental realization, and photon-pair correlations with phase mismatch.
- [20] F. Setzpfandt, A. A. Sukhorukov, D. N. Neshev, R. Schiek, Y. S. Kivshar, and T. Pertsch, *Phys. Rev. Lett.* **105**, 233905 (2010).
- [21] H. Y. Leng, X. Q. Yu, Y. X. Gong, P. Xu, Z. D. Xie, H. Jin, C. Zhang, and S. N. Zhu, *Nature Commun.* **2**, 429 (2011).
- [22] A. Rossi, G. Vallone, A. Chiuri, F. De Martini, and P. Mataloni, *Phys. Rev. Lett.* **102**, 153902 (2009).
- [23] P. L. de Assis, M. A. D. Carvalho, L. P. Berruezo, J. Ferraz, I. F. Santos, F. Sciarrino, and S. Padua, *Opt. Express* **19**, 3715 (2011).